The Canadian Mineralogist
Vol. 43, pp. 183-202 (2005)

RECRYSTALLIZATION TEXTURES IN ZIRCON GENERATED BY OCEAN-FLOOR AND ECLOGITE-FACIES METAMORPHISM: A CATHODOLUMINESCENCE AND U–Pb SHRIMP STUDY, WITH CONSTRAINTS FROM REE ELEMENTS

Encarnación PUGA[§]

Instituto Andaluz de Ciencias de la Tierra, CSIC–UGRA, Facultad de Ciencias.
Avda. Fuentenueva s/n, E–18002 Granada, Spain

C. Mark FANNING

Research School of Earth Sciences, The Australian National University, Mills Road, Canberra ACT 0200, Australia

José Miguel NIETO

Departamento de Geología. Facultad de Ciencias Experimentales, Universidad de Huelva.
Avda. Fuerzas Armadas s/n, E–21071 Huelva, Spain

Antonio DÍAZ DE FEDERICO

Departamento de Mineralogía y Petrología. Facultad de Ciencias, Universidad de Granada.
Avda. Fuentenueva s/n, E–18002 Granada, Spain

Abstract

Eclogites formed during the Eo-alpine metamorphic event are common within the ophiolitic unit of the Mulhacén complex, which forms part of the Betic Cordillera in southeastern Spain. A detailed study with cathodoluminescence (CL) images of zircon from these eclogites has revealed three types of domains, confirmed by some differences in their REE patterns and ages. There are a) igneous domains, with oscillatory zoning, yielding an Early to Middle Jurassic age, dating the crystallization of the basic protolith, and b) two different types of recrystallized metamorphic domains, one with grey homogeneous CL images, mainly clustering around the Late Jurassic, and the other with bright clouded CL images, ranging down to a Late Cretaceous to Paleocene age. These two types of recrystallized areas in the zircon are interpreted as having formed during the ocean-floor and the Eo-alpine metamorphism, in eclogite-facies conditions, respectively. We contend that processes of metamorphic recrystallization, which are more pervasive in the internal part of the zircon crystals than at their edge, was facilitated by oceanic fluids that circulated through them and were located in their vesicles, forming fluid inclusions

Keywords: U–Pb SHRIMP dating, zircon, REE analyses, recrystallization textures, eclogites, ophiolites, ocean-floor metamorphism, Alpine metamorphism, Betic Cordillera, Spain.

Sommaire

Les éclogites formées lors de l'événement métamorphique éo-alpin sont répandues dans l'unité ophiolitique du complexe de Mulhacén, dans la Cordillère Bétique du sud-est de l'Espagne. Nous avons utilisé les images en cathodoluminescence du zircon dans ces éclogites pour documenter trois types de domaines, distingués par leurs enrichissement en terres rares et leurs âges. Il y a d'abord les domaines ignés, avec zonation oscillatoire, qui donnent un âge jurassique précoce à moyen et fixent ainsi l'âge de cristallisation du protolithe basique, et ensuite deux sortes de domaines recristallisés lors du métamorphisme, un avec une cathodoluminescence grise homogène, qui donne un âge jurassique tardif en moyenne, et l'autre avec une cathodoluminescence brillante mais embrouillée, qui donne un âge plus jeune, allant de crétacé tardif à paléocène. Ces deux types de domaines recristallisés du zircon se seraient formés au cours du métamorphisme sur le fonds océanique et le métamorphisme éo-alpin sous conditions du faciès éclogite, respectivement. Nous croyons que les vacuoles dans le zircon ont favorisé la circulation de l'eau, fixée en partie sous forme d'inclusions fluides, ce qui rend compte de la recristallisation plus avancée dans le coeur des cristaux que le long de leur bordure.

(Traduit par la Rédaction)

Mots-clés: datation U–Pb avec la technique SHRIMP, zircon, analyses pour les terres rares, textures de recristallisation, éclogites, ophiolites, métamorphisme des fonds marins, métamorphisme alpin, Cordillère Bétique, Espagne.

§ *E-mail address*: epuga@ugr.es

Introduction

Basic magmatism developed at the proto-realm of the Betic Cordillera during a period of extension in Triassic and Jurassic times. This period led to the opening of the western-end branch of the Tethys Ocean and its connection with the central Atlantic, which separated the Eurasian and African plates (Andrieux *et al.* 1989, Favre & Stampfli 1992, Guerrera *et al.* 1993, Vera 2001, Puga, in press). Subvolcanic and submarine volcanic rocks, with tholeiitic to slightly sodic-alkaline compositions, were generated by the partial melting of a lithospheric mantle under within-plate extensional conditions in different zones of the Betic Cordillera (Puga & Torres Roldán 1989, Puga *et al.* 1989a, Morata *et al.* 1997). The only exception to the subcontinental origin of this magmatism (until now recognized geochemically) is provided by the eclogites of the Mulhacén complex (MC) (Fig. 1), which crop out as numerous tectonic lenses genetically associated with ultramafic rocks and metasedimentary units. These lithologies made up a dismembered and metamorphosed ophiolitic sequence, which was defined by Puga (1990) as the Betic Ophiolitic Association (BOA). This oceanic magmatism has been dated as Jurassic by: K–Ar (Portugal *et al.* 1988), Rb–Sr (Hebeda *et al.* 1980) and Ar–Ar (De Jong 2003). However, these radiogenic systems may record variable open-system behavior during the polyphasic Alpine metamorphism that affected the rocks. The presence of excess argon in some K-bearing minerals is considered likely. In order to remove possible ambiguities in the Rb–Sr, K–Ar and Ar–Ar age data, SHRIMP (sensitive high-resolution ion microprobe) U–Pb analyses of zircon, in conjunction with cathodoluminescence (CL) imaging, provides a reliable means of determining the ages of crystallization of magmatic rocks, even those that have been affected by metamorphism. Through the CL images, one can identify simple zoned magmatic zircon, and also zircon that has been subjected to new growth, or recrystallization during the high-grade metamorphism.

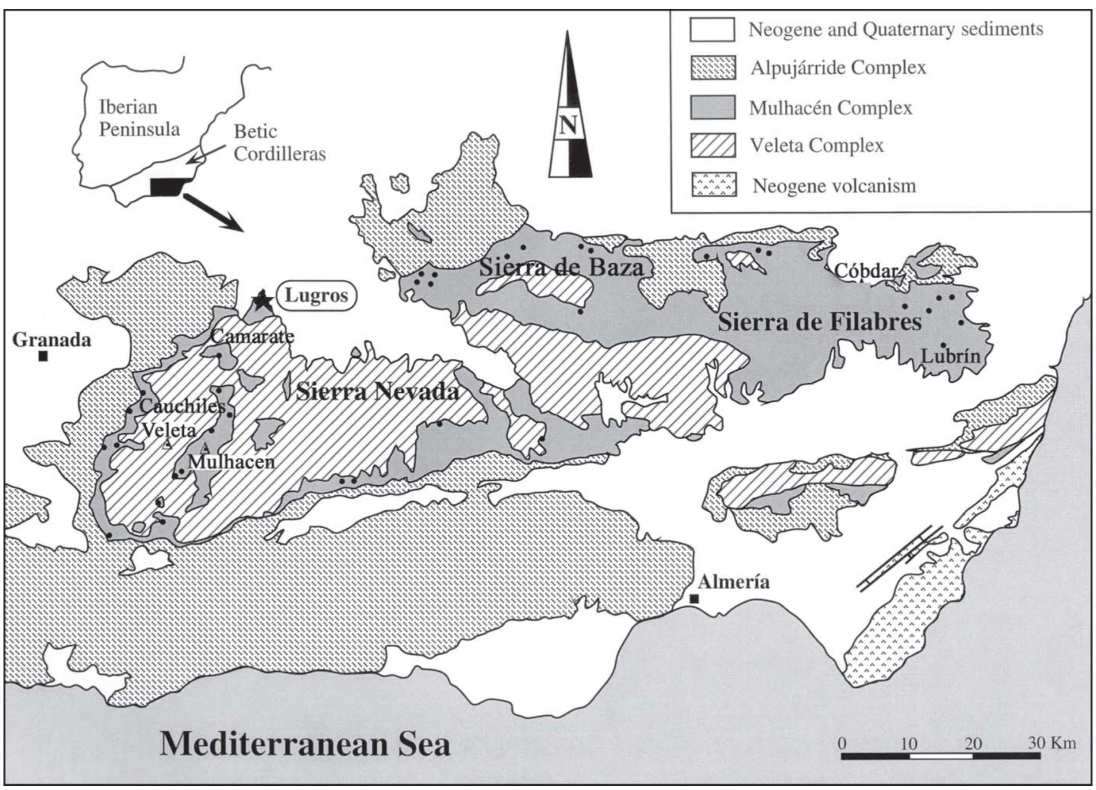

FIG. 1. Geological sketch-map of the central-eastern sector of the Betic Cordilleras, showing the main part of the Mulhacén complex. Black dots represent the largest outcrops of the Betic ophiolitic association located along Sierra Nevada, Sierra de Baza and Sierra de Filabres. The black star indicates the location of the Lugros eclogite outcrop from which the zircon crystals dated by SHRIMP were taken.

As part of a (SHRIMP) U–Pb study of zircon in the igneous and sedimentary protoliths of the MC ophiolites, we have identified in the Lugros eclogites some crystals of zircon that preserve igneous zonal growth, enabling us to date with precision the age of this magmatism. There are also recrystallized zones that yield some information on the timing of the metamorphic processes that have overprinted the magmatic rocks. The recrystallized zones show with CL some curious textures different from those previously described in recrystallized zircon. The principal aims of this paper are to document the recrystallization-induced textures of the zircon with cathodoluminescence (CL) images, present the U–Pb dating and REE analyses of their various texturally distinct zones, and to explore the possible correlation of the evolution of zircon crystals with the successive metamorphic processes registered in their host eclogites.

Geological Outline of the Betic Cordillera

The Betic Cordillera forms the westernmost part of the Mediterranean Alpine chains and crop out in southern Spain as a relatively continuous band of about 600 km in length and 200 km wide (Fig. 1). This cordillera is divided into a northern external domain, the Prebetic and Subbetic zones, and a southern internal domain, the Betic Zone. The Betic External Zones consist of Triassic to Middle Miocene mainly sedimentary rocks, which were deposited on the southern Iberian continental margin. The Betic Internal Zone is an allochthonous terrane, derived from the Meso-mediterranean microplate, and comprises several tectonic complexes of mainly metamorphic rocks of Paleozoic to Tertiary age (Vera 2001, and references therein).

The Internal Zone of this cordillera has generally been subdivided into three nappe complexes. They are, from bottom to top: the Nevado–Filábride, Alpujárride and Maláguide. They are in some cases respectively correlated with the Penninic, lower Austro-alpine and upper Austro-alpine nappes of the Alps (Torres Roldán 1979, Michard *et al.* 1991). The Nevado–Filábride Complex has been further subdivided into the Veleta and the Mulhacén complexes (Puga *et al.* 2002a).

The Veleta Complex (VC) is the deepest of the Internal Zones of the Betic Cordillera. It crops out only in the central and eastern sectors of the Betic Cordillera, forming a series of tectonic windows overlain by the Mulhacén Complex (MC) (Figs. 1, 2). The VC has been overthrust by the MC at the end of the Late Cretaceous–Paleocene Eo-alpine metamorphic event and by the Alpujárride and Maláguide complexes after the Eocene–Oligocene Meso-alpine event (Torres Roldán 1979, Puga *et al.* 2002a, and references therein).

The VC is mostly comprised of several thousand meters of graphite-bearing micaschists alternating with quartzite layers more abundant toward the top of the complex. These lithologies constitute a Paleozoic and probably more ancient basement, which is overlain by the San Francisco unit, made up of chloritoid- and kyanite-bearing micaschists and quartzites. The latter probably represents a Permo-Triassic cover. The record of the Pre-alpine metamorphism in this complex has been nearly obliterated by the Alpine metamorphism, which evolved from the albite–epidote amphibolite- to greenschist-facies conditions during Eo-alpine to Meso-alpine events.

The MC is composed of two thrust units of crustal origin, the Caldera below and the Sabinas above, between which the oceanic Ophiolite unit is tectonically intercalated (Fig. 2). The crustal units are made up of a Paleozoic basement, which consists primarily of graphite-bearing micaschists containing slices of metagranite and eclogitized skarn-rocks, and a Mesozoic cover, mainly composed of marble, micaschists and rhyolitic orthogneisses. In the Caldera unit, the Pre-alpine assemblages, formed at conditions of the almandine amphibolite facies, were only partly obliterated by the Alpine assemblages.

The Ophiolite unit comprises numerous meter- to kilometer-size lenses of metamorphic rocks, derived from mafic, ultramafic and sedimentary rock-types, with mylonitic fabrics near the contacts with other Mulhacén nappes (Puga 1990). This ophiolite unit is dismembered and metamorphosed in the same way as its counterparts in the Pennine nappes of the Alps (Dal Piaz 1974, Dietrich 1980, Beccaluva *et al.* 1984, Desmons 1989), and it is discontinuously exposed along *ca*. 250 km in the MC (black dots in Fig. 1).

The Alpine metamorphism in the MC developed under eclogite-facies conditions during the first Alpine metamorphic event (Eo-alpine), and under conditions of the albite–epidote amphibolite facies in the second (Meso-alpine) event. The only exception to this metamorphic evolution is represented by the Soportújar Formation, formed by discontinuous horizons of continental and evaporitic metasedimentary and metatuffitic rocks, which were deposited upon different units of the MC between the Eo-alpine and Meso-alpine events. This formation contains only albite–epidote amphibolite or greenschist assemblages formed during the Meso-alpine metamorphic event (Puga *et al.* 1996). In the MC, the Early Miocene Neo-alpine event locally gave rise to greenschist-facies parageneses owing to retrogression of the Eo-alpine and Meso-alpine assemblages (Puga *et al.* 2000, 2002a).

The subdivision of the Alpine orogeny in the MC into the successive metamorphic events: Eo-alpine, Meso-alpine and Neo-alpine, separated by stages of relaxation, is based on the metamorphic and deformational evolution of their different rock-types and on radiometric dating (Puga *et al.* 2002a, and references therein). This subdivision is also consistent with the model for the Cenozoic kinematic evolution of the Western Mediterranean oceanic basins and their peripheral orogens established by Dewey *et al.* (1973, 1989). From the magnetic anomalies in the central and northern Atlantic Ocean, these authors deduced the relative path of motion between European and African plates and microplates. They recognized a period of extension from Late Triassic to Cenomanian, followed by two main periods of compression separated by a Paleocene to Early Eocene stage of restoration. During the first period of extension, the basic magmatism in the External and Internal Zones of the Betic Cordillera developed, including the formation of the band of ocean floor from which the MC ophiolites were derived, which connected the Ligur–Piemontes Ocean with the Central Atlantic (Puga *et al.* 2002a, Puga, in press). Subduction of this oceanic floor together with the continental margins took place during the first period of compression, giving rise to the Eo-alpine metamorphic event, in the eclogite-facies conditions (Puga *et al.* 2002a). A part of the subducted formations were exhumed during the ensuing stage of restoration. The intra-orogenic Soportújar Formation was then laid down, owing to erosion of the exhumed eclogitic rocks and by comtemporaneous andesitic magmatism, genetically related to the Eo-alpine subduc-

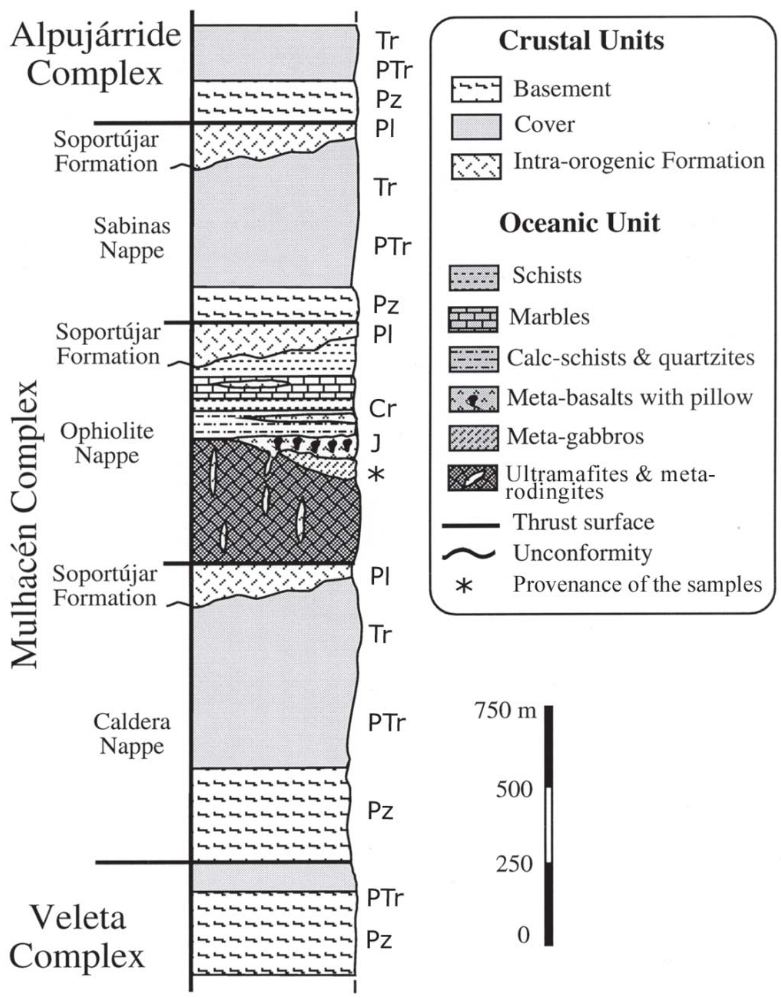

FIG. 2. Simplified lithostratigraphic column of the metamorphic complexes represented in Figure 1, showing the main rock-types of the BOA in a reconstruction of their relative position during the primitive oceanic stage. The most probable ages, inferred from radiometric and paleontological data for the different formations making up this column, are indicated as follow: Pz: Paleozoic, PTr: Permo-Triassic, Tr: Triassic, J: Jurassic, Cr: Cretaceous, Pl: Paleocene. The star indicates the lithostratigraphic provenance of the eclogites containing the dated crystals of zircon.

tion (Puga *et al.* 1996). The Meso-alpine event occurred during the following period of compression, and this was probably accompanied by an intracrustal subduction, which ended with the continental collision of the Iberian and African plates. This second metamorphic event attained a climax in the Late Eocene, under conditions of the albite–epidote amphibolite facies, and was followed by an Oligocene stage of extension under greenschist-facies conditions (Puga *et al.* 2002a). Very scarce blastesis, mainly at greenschist-facies conditions, took place during the Miocene Neo-alpine event in the MC. The Miocene radiometric ages recorded in some rocks have been interpreted as reflecting partial re-opening of the isotopic systems, most probably related to late stages of extensional tectonics (Monié *et al.* 1991). Alternatively, these young ages may be related to the volcanic activity that generated the Cabo de Gata volcanic province, as well as the associated hydrothermal alteration and mineralization in the nearby metamorphic rocks (Bellon *et al.* 1983, De Jong *et al.* 1992).

Petrological and Geochemical Characteristics of the Betic Ophiolites and Previous Geochronological Constraints

Figure 2 shows a hypothetical reconstruction of the Betic Ophiolites (BOA) which, in terms of primary rocks, is formed from bottom to top by: 1) an ultramafic sequence, consisting of serpentinized lherzolites, from several meters up to 500 meters thick, containing numerous boudinaged dolerite dykes, 2) a layered plutonic sequence made up of cumulus troctolites and gabbros cross-cut by dolerite dykes, 3) a volcanic sequence composed of basalts with pillow structures, lying unconformably on top of the plutonic sequence, 4) a metasedimentary sequence made up mainly of ankerite-bearing calc-schists (locally preserving scarce relics of Cretaceous foraminifera), with some micaschist, quartzite and marble layers. This sequence may be found directly overlying the ultramafic or the basic sequence, as indicated in Figure 2.

The ultramafic rocks of the Ophiolite Unit are mainly serpentinites, derived from spinel lherzolites and secondary harzburgites with a spinifex-like texture. They contain abundant doleritic dykes, partly rodingitized, which locally preserve an E–MORB chemical affinity. The rodingitization process that affected the dolerite dykes, highlighted mainly by a significant increase in Ca content, is coeval with, and complementary to, an oceanic serpentinization process that depleted Ca in some of the host lherzolites through the breakdown of clinopyroxene. These serpentinized lherzolites were transformed into secondary harzburgites, with pseudo-spinifex textures, during the high-pressure Eo-alpine metamorphic event, whereas the dolerite dykes were transformed into eclogites (Puga *et al.* 1999a, Ruiz Cruz *et al.* 1999).

The basic rocks of the Ophiolite Unit locally preserve igneous parageneses showing a crystallization sequence consisting of: spinel → olivine → plagioclase → clinopyroxene → apatite → Fe–Ti oxides, which corresponds to that of a tholeiitic magma. Despite their metamorphic transformation, the chemical composition of these metabasic rocks is similar to that displayed by current E–MORB-type magmas. Moreover, their initial ^{143}Nd–^{144}Nd isotopic value, *ca.* 0.5130, and ^{87}Sr– ^{86}Sr value, *ca.* 0.703, also correspond to magmatism generated in a MORB geodynamic setting (Saunders *et al.* 1988).

The various igneous lithotypes comprising the BOA preserve chemical and mineralogical evidence of a metasomatic and metamorphic recrystallization prior to the development of the Alpine orogenic metamorphism. During this oceanic stage, high-gradient amphibolite- and greenschist-facies metamorphic assemblages formed in both the gabbros and basalts of this association, of which only relics have been preserved (Puga *et al.* 1999b, 2002b). The saline hydrous fluids active during this oceanic stage could explain the high chlorine content present as submicroscopic inclusions of NaCl in some metasomatized igneous minerals, such as olivine (Puga *et al.* 1999b), as well as in the mineral phases newly formed during this stage, such as brown amphibole, sodic-calcic plagioclase and phlogopite, among others (Puga *et al.* 2002b). These saline fluids may also have facilitated the development of the recrystallized textures present in the zircon.

The radiometric data previously published on the BOA rocks are presented in Table 1, and a discussion of these and other radiometric data on the MC and VC rocks is given in Puga *et al.* (2002a).

The metabasic rocks of the BOA have Rb–Sr, K–Ar and ^{40}Ar–^{39}Ar dates that straddle the Triassic–Jurassic boundary, ranging to the Late Jurassic. Moreover, ^{40}Ar–^{39}Ar laser-probe dating of brown amphiboles, filling millimetric veins in the Cóbdar ophiolitic metabasalts (Puga *et al.* 2002b), yielded a Late Jurassic date for the oceanic metamorphism, coeval with, or slightly younger than, the Late Jurassic volcanic activity (Puga *et al.* 2002a).

Radiometric dating of associations of metamorphic minerals that developed during the Alpine orogeny in the BOA rocks are scarce. The interpretation is in some cases ambiguous, mainly owing to the possible existence of excess Ar in K-bearing minerals (Puga *et al.* 2002a, De Jong 2003) and to the Sm–Nd isotopic disequilibrium observed in eclogitic assemblages (Nieto *et al.* 1997). Nevertheless, three events of Alpine metamorphism can be envisaged, as for the other units of the MC, on the basis of the available data on K–Ar, ^{40}Ar–^{39}Ar and U–Pb, obtained on mineral separates using a SHRIMP instrument.

Petrology of the Zircon-Bearing Protoliths and Field Occurrence

The eclogite lenses selected for this study crop out near the village of Lugros to the north of Sierra Nevada (Fig. 1). These eclogites form three tectonic klippen several hundred meters to 1 km in length and less than 100 meters thick, thrust over garnet-bearing micaschists of the Caldera unit and covered by Quaternary deposits. The Lugros eclogites are derived from volcanic and predominantly plutonic protoliths cut by scarce decimetric dykes of dolerite. The plutonic protoliths consist mainly of gabbro, some olivine-bearing, with a medium- to coarse-grained doleritic and locally pegmatitic texture. The volcanic sequence is mainly restricted to loose blocks within an outcrop several hundred meters in extent. Most of these blocks comprise multiple, irregularly folded layers of basalt, several centimeters in thickness, with a quenched outer part, an aphyric black intermediate zone, and a hypocrystalline central zone. Other blocks in the Lugros suite are formed by piles of molded minipillows, several centimeters in diameter, alternating with other drained pillow structures several decimeters in maximum length. All these structures are the result of submarine eruptions involving recurrent small volumes of highly fluid magma, giving rise to lavas predominantly with small pillows and flow structures, which are locally very well preserved despite the orogenic metamorphism (Puga *et al.* 1995).

TABLE 1. PREVIOUS GEOCHRONOLOGICAL DATA ON METABASIC ROCKS AND MICASCHISTS OF THE BETIC OPHIOLITIC ASSOCIATION (BOA), SPAIN

Type of sample	Locality	Method	Closure age (Ma)	Reference
		Jurassic magmatism		
Intercumulus biotite in gabbro	Cóbdar	$^{40}Ar–^{39}Ar$	213 ± 2.5	Puga *et al.* (1991)
Gabbro (WR)	Cóbdar	K–Ar	174 ± 4	Portugal *et al.* (1988)
Biotite relic in metagabbro	Lubrín	$^{40}Ar–^{39}Ar$	173 ± 6	De Jong (2003)
Relict igneous plagioclase in dolerite	Cóbdar	K–Ar	164 ± 4	Portugal *et al.* (1988)
Ocean-floor metamorphic amphibole in basalt	Cóbdar	$^{40}Ar–^{39}Ar$ laser probe	158 ± 4	Puga *et al.* (1991)
Olivine dolerite mineral isochron	Lubrín	Rb–Sr	146 ± 3	Hebeda *et al.* (1980)
		Eo-Alpine event		
Phengite	Lubrín	$^{40}Ar–^{39}Ar$	86.2 ± 2.4	De Jong (2003)
Glaucophane	Cóbdar	K–Ar	72 ± 1	Portugal *et al.* (1988)
		Meso-Alpine event		
Barroisitic amphibole	S^{a} Baza	Ar–Ar	48.4 ± 2.2	Monié *et al.* (1991)
Barroisite	Cóbdar	Ar–Ar	41.4 ± 2.3	Puga *et al.* (2002a)
White mica	Cauchiles	Ar–Ar	28.5 ± 2.5	Puga *et al.* (2002a)
Phengitic mica	Cóbdar	K–Ar	27± 1	Portugal *et al.* (1988)
Magnesio-hornblende	S^{a} Baza	Ar–Ar	24.6 ± 3.6	Monié *et al.* (1991)
		Neo-Alpine event		
Zircon	Almirez	U–Pb SHRIMP	15.0 ± 0.6	López Sánchez-Vízcaino *et al.* (2001)
White mica	Cauchiles	Ar–Ar	13.0 ± 1.5	Puga *et al.* (2002a)
Paragonite	Camarate	Ar–Ar	12.4 ± 1.1	Puga *et al.* (2002a)
Actinolite	Almirez	K–Ar	11 ± 3	Portugal *et al.* (1988)
Actinolite	Camarate	Ar–Ar	11± 0.9	Puga *et al.* (2002a)

Igneous textures are preserved in the Lugros gabbros, but the igneous parageneses were entirely transformed into kyanite-bearing eclogite, and less commonly into co-facial garnet glaucophanite during the intra-oceanic subduction process of the Upper Cretaceous – Paleocene Eo-alpine event. Relics of brown amphibole, similar to that formed during oceanic metamorphism in the Cóbdar ophiolites (Puga *et al.* 2002b), are present in some samples. This mineral contains abundant tiny crystals of exsolved rutile and shows a gradual transition to green sodic-calcic amphibole that occurred during subsequent orogenic stages. The igneous paragenesis, now represented mainly by pseudomorphs of plagioclase, clinopyroxene, olivine and ilmenite, was also pervasively transformed during the prograde stage of the Eo-alpine event. Zircon is a minor phase in the igneous paragenesis, but it is not easily identified under the microsope owing to its small size. The primary olivine surrounded by calcic plagioclase was replaced by aggregates of omphacite rimmed by almandine, forming a coronitic texture. Clinopyroxene was transformed into omphacite + rutile, and calcic plagioclase was replaced, during the prograde stage, firstly by clinozoisite–paragonite intergrowths, and later by omphacite + kyanite aggregates. Ilmenite is replaced by rutile aggregates. Centimetric veins filled with kyanite ± omphacite may be found in these eclogites (Puga *et al.* 1995). The conditions of the metamorphic climax deduced for the Eo-alpine event in Lugros outcrop correspond to *ca.* 21–22 kbar and 700°C (Puga *et al.* 2000).

During the retrograde Eo-alpine stage, which took place during the partial exhumation of the previously subducted ocean floor toward the surface, some hydrous minerals developed, mainly in the pressure shadows of the eclogitic poikiloblasts and partly replacing them. The most peculiar mineral of this stage is glaucophane, which replaces omphacite and garnet, although some crystals may also be found as inclusions in these eclogitic minerals. Albite, epidote, phengite, paragonite and chlorite coexist, in minor proportions, with glaucophane, formed in the glaucophane schist facies during this retrograde stage.

In the Lugros outcrop, the Eo-alpine parageneses were only slightly overprinted by the albite–epidote amphibolite assemblages during the Meso-alpine event. Omphacite, previously developed at the expense of different igneous microdomains, was first partially replaced by an amphibole–albite symplectitic intergrowth, and later by sodic-calcic amphiboles, mainly barroisite, katophorite, taramite and edenite. These amphiboles, together with epidote and minor albite, phengite and chlorite, also replace the eclogitic garnet, forming coronas at their periphery and penetrating along fissures. Rutile is partly replaced and overgrown by titanite. Glaucophane and minor chlorite of the retrograde Eo-alpine stage were pervasively transformed and overgrown by the sodic-calcic Meso-alpine amphiboles, which developed at T conditions clearly higher than glaucophane in these rocks (Puga *et al.* 2000). The Meso-alpine metamorphic conditions correspond to the albite–epidote amphibolite facies, with a retrograde stage under greenschist-facies conditions. The metamorphic climax conditions deduced for this event attained *ca.* 600°C and 9 kbar (Puga *et al.* 2000).

Textural Characteristics of the Zircon

The zircon crystals in the Lugros eclogites are scarce and vary in size from approximately 20 to 100 μm across. The grains (Figs. 3, 4) are mostly subhedral to euhedral; some grains are skeletal or hopper-shaped, interpreted to reflect rapid growth (Naslund 1984). A few crystals show sinuous connections that extend from the outer face of a crystal to the center of the grain (crystals 2 and 8, Fig. 4). The CL images reveal the true complexity of the internal structures; a significant component shows oscillatory zoning, interpreted to be igneous in origin (*cf.* Vavra 1990, Pidgeon 1992). In many cases, the internal parts of the grains have a more irregular CL response, and appear as clouded areas of bright CL. We have distinguished three types of zone within these crystals according to their luminescence, their shape, and mutual spatial relationships (Figs. 3, 4): 1) Type-I zones correspond to the relatively subordinate areas with oscillatory zoning near the idiomorphic rim (crystals B, C in Fig. 3, and 1, 2, 4, 5 in Fig. 4). They have been interpreted as being igneous in origin. 2) Type-II zones are formed of light grey, more-or-less homogeneous areas, which are commonly present from the edge to the core of the zircon crystal (Figs. 3, 4). These CL grey unzoned areas are well represented in A, C and F crystals in Figure 3, although they also occupy minor areas in the other crystals shown in Figures 3 and 4. 3) Type-III zones correspond to the brightest CL areas in these crystals; they show very irregular shapes, and are more abundant toward the center than at the periphery of the crystals (A, B, F in Fig. 3, and 4, 5, 8 in Fig. 4), although they are also present in the majority of the irregular rim (C, D, E in Fig. 3, and 1, 7 in Fig. 4). These zones, with strong luminescence, commonly surround holes (black in the CL image), as can be seen in all crystals shown in Figures 3 and 4.

The oscillatory-zoned areas within these grains are interpreted as representing igneous zircon formed during magmatic crystallization. The grey homogeneous and clouded areas, assigned to types II and III above, are interpreted as reflecting an alteration of this primary zircon, presumably by recrystallization under the influence of fluids. The abundance of holes and cavities is relatively common in zircon that has grown quickly. These holes most probably acted as conduits for the internal movement of the oceanic fluids, located in vesicles, facilitating the later recrystallization of the zircon during metamorphic processes.

These textures differ from those arising from recrystallization processes in granulite facies as described by Vavra *et al.* (1996) and Hoskin & Black (2000, and references therein). However, they seem similar to textures present in zircon of Alpine eclogites, dated by Rubatto *et al.* (1998) and Rubatto & Hermann (2003), which they interpreted to indicate alteration zones due to fluid percolation along microfractures.

Geochronology

The U–Pb data for the zircon crystals shown in Figures 3 and 4 are presented in Table 2 and plotted on Figure 5, a Tera & Wasserburg concordia plot of the total ratios, calibrated for U–Pb, but uncorrected for common Pb. For the current study, 36 areas have been analyzed on 22 grains from sample ELUG 61 using the sensitive high-resolution ion microprobe (SHRIMP) at the Australian National University of Canberra, using methods described by Williams (1998, and references therein). The selection of the zircon crystals for SHRIMP analyses was done on the basis of the CL images. One of the key aims was to constrain the age of the Eo-alpine metamorphic event developed in eclogite-facies conditions.

On the Tera & Wasserburg plot (Fig. 5), many of the data points plot well above the concordia curve, a consequence of high amounts of common Pb, attaining approximately 15% for values represented in Table 2. There is also considerable scatter of analytical data; a dominant, coherent group gives ^{206}Pb–^{238}U ages of about 180–190 Ma. A second, subordinate group appears to indicate about 150 Ma, with the remaining data showing no unique or coherent pattern of ages, trailing off to what are considered to be discordant data, with ^{206}Pb–^{238}U ages as young as ~30 Ma (Table 2, Fig.5).

The oscillatory-zoned areas (Type I) comprise the coherent grouping on this plot, and this is further highlighted on the probability–density plot, with a stacked histogram, shown as inset on Figure 5. A weighted mean of the ^{206}Pb–^{238}U ages for nine oscillatory-zoned areas gives 184 ± 4 Ma (MSWD = 2.3), interpreted as the age of magmatic crystallization. We have not identified texturally (or dated) any overgrowths, nor have we found any inherited cores older than the early Jurassic ages provided for the zoned igneous zircon (Type I).

Analyses of the homogeneous grey zones (type II) and of the bright CL, mottled areas (Type III), yield a wide range of ^{206}Pb–^{238}U ages. Four of these appear to form a fairly coherent grouping, with ^{206}Pb–^{238}U ages at *ca.* 150 Ma (Fig. 5).

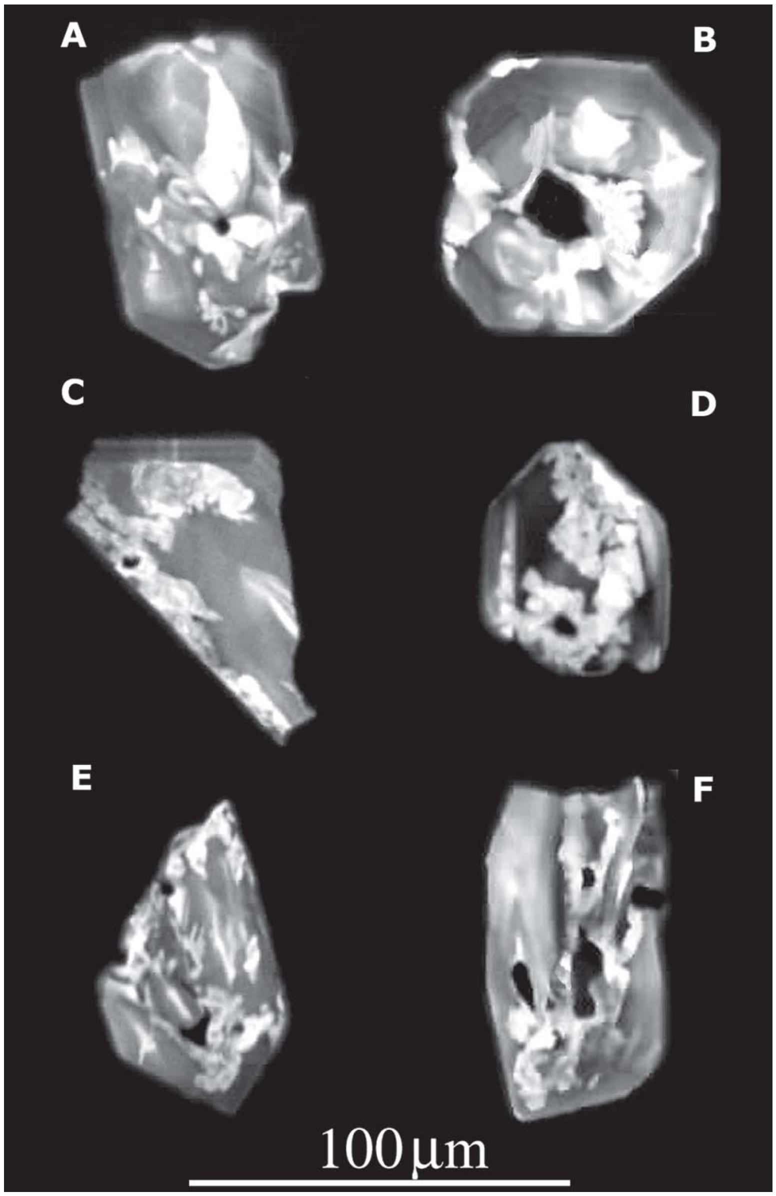

FIG. 3. Cathodoluminescence photos of the most peculiar textures presented by zircon crystals in the Lugros eclogites, generated by recrystallization processes, plausibly facilitated by fluids filling vesicles. Photos A and B show a "corona" texture, with the brightest areas spreading outward from a central vesicle. In photos C and D, the shape of the brightest areas resembles a "cloud of smoke" rising from the vesicle. In photos E and F, the brightest spots have the appearance of "flames", both joined to and separate from the visible vesicles in the host zircon.

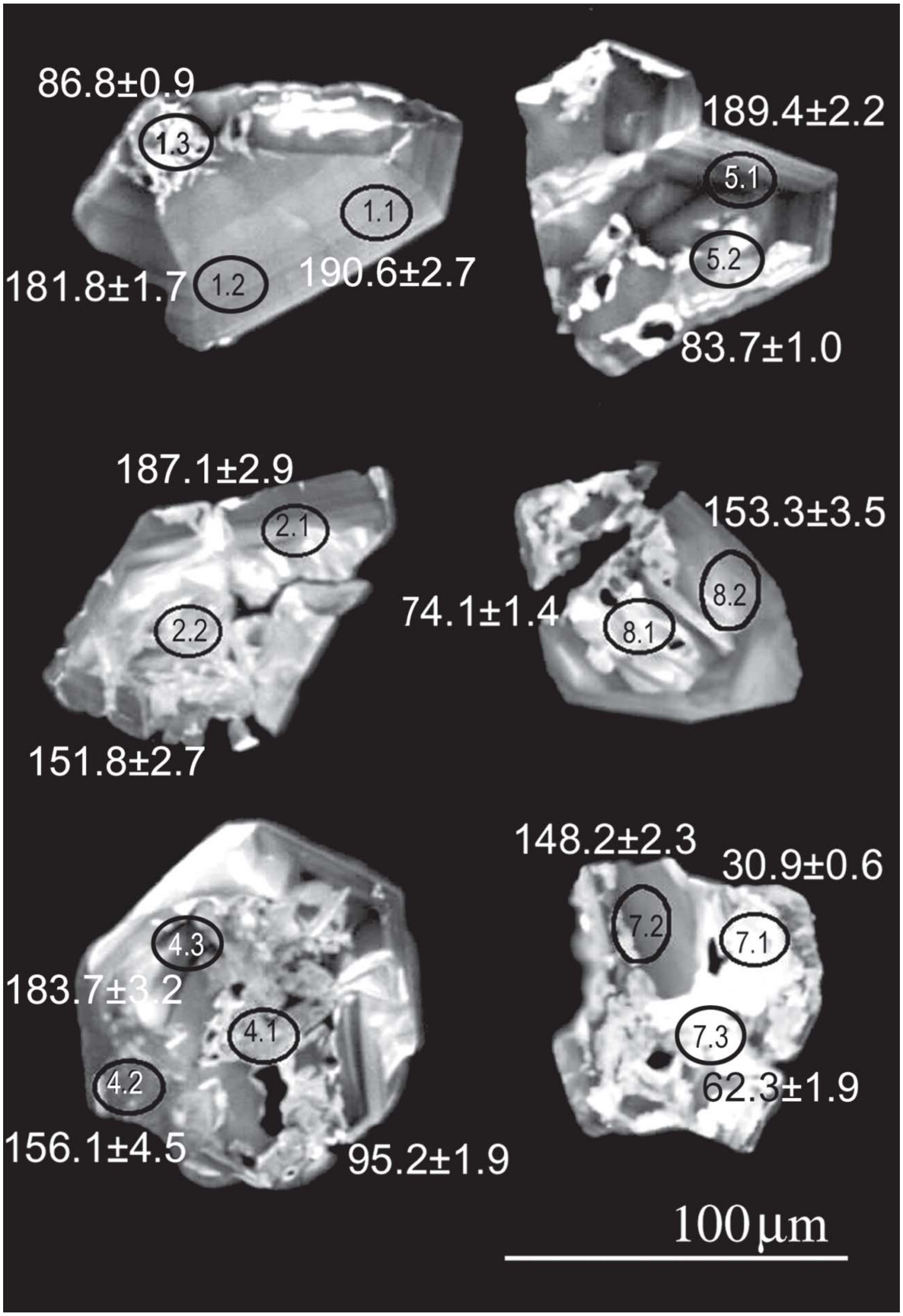

FIG. 4. Representative CL images of zircon crystals dated in this study. Numbers in circles refer to analysis number in Table 2 and Figure 6.

The analyses of the Type-III zircon areas did not yield any coherent data on ages. In fact, the bright recrystallized zones around internal holes and cavities of these zircon crystals yielded scattered and discordant apparent ages, ranging mainly from Late Cretaceous to Paleocene times (Fig. 5). They are interpreted to represent incomplete resetting of U–Pb isotopic compositions due to varying degrees of partial recrystallization.

A detailed examination of the areas analyzed in terms of their U and Th concentrations shows that in general, the recrystallized areas (types II and III) contain less U and Th and also have a lower Th/U value than the igneous areas (type I) of the same crystal (Table 2, Fig. 6). This is clearly shown in crystals such as number 4 (Fig. 6), in which it has been possible to analyze the three type of areas. An exception is presented by the recrystallized area, spot 1.3 in crystal 1, that contains higher levels of U and Th than the oscillatory-zoned area, spot 1.1 of the same crystal, although the Th:U ratio also decreases from spot 1.1 to 1.3 (Fig. 6). The decrease in Th/U value from igneous protolith to recrystallized areas in the zircon crystals of the Lugros eclogites is, however, less than what usually is found in newly formed zircon. In fact, the Th/U value in the recrystallized areas of zircon shown in Figure 6 and Table 2 ranges from about 0.8 to 0.1, whereas in newly formed metamorphic zircon of eclogites from the Western Alps, this ratio is about 0.01 (Rubatto 2002).

The high Th and the increase in Th/U shown by some of the brightest areas, mainly present in spots 7.1 and 7.3 (Type III) with respect to spot 7.2 (Type II), and also present to a lesser extent between spot 8.1 with respect to 8.2 (Fig. 6), might be better explained by a local chemical re-equilibration due to the breakdown of some Th-rich mineral phase (*e.g.*, allanite or clinozoisite) near these zircon crystals during a recrystallization process associated with inferred percolation of fluid.

Analyses of the Zircon for the Rare Earths and Other Trace Elements

Analyses of the zircon for the rare-earth elements, Y and Hf were made on most of the areas used for the U–

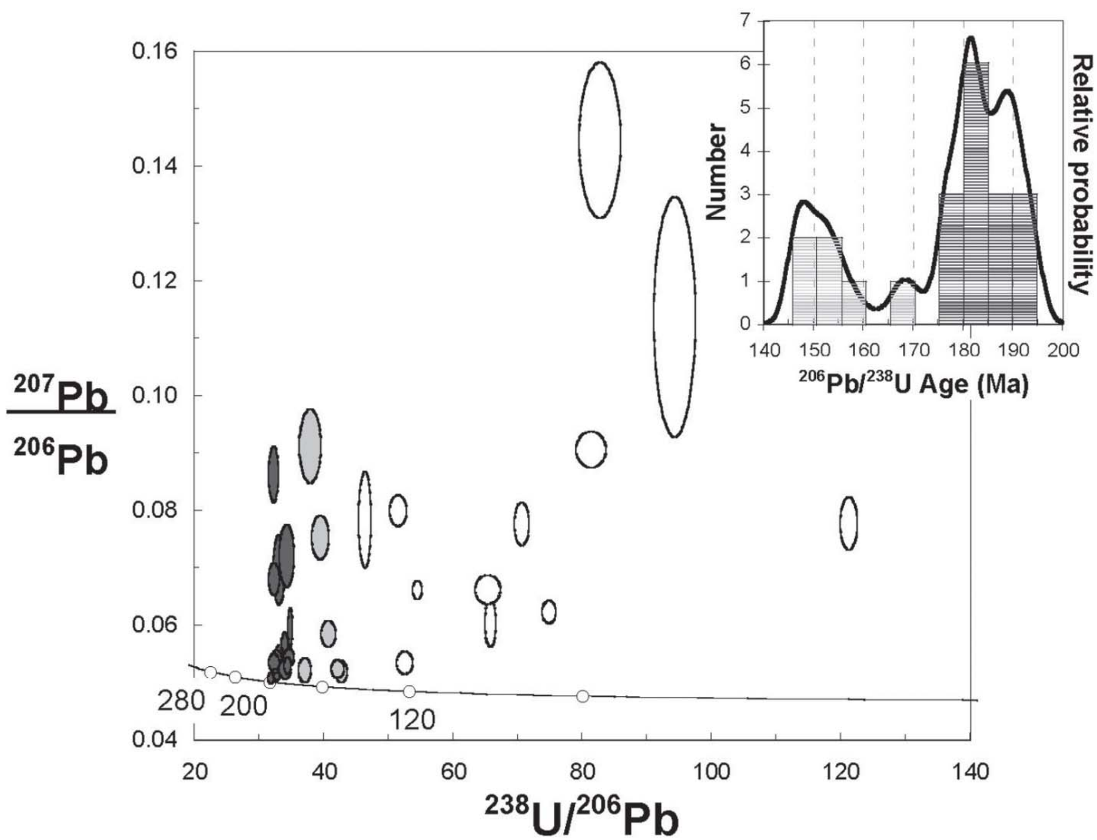

FIG. 5. Tera-Wasserburg diagram for the zircon crystals analyzed. Analytical results are shown as one-sigma error ellipses, plotted as total ratios, calibrated, but uncorrected for common Pb.

TABLE 2. SUMMARY OF SHRIMP U–Pb ZIRCON RESULTS FOR THE CRYSTALS SHOWN IN FIGURE 4 AND REFERRED TO IN FIGURES 6 AND 7

								Total				Radiogenic		Age (Ma)	
Gr. spot	Type	U ppm	Th ppm	Th/U	Pb* ppm	$^{204}Pb/^{206}Pb$	f_{206} %	$^{238}U/^{206}Pb$	±	$^{207}Pb/^{206}Pb$	±	$^{206}Pb/^{238}U$	±	$^{206}Pb/^{238}U$	±
1.1	I	394	458	1.16	13	0.000266	0.226	33.244	0.470	0.0517	0.0008	0.0300	0.0004	190.6	2.7
1.2	I	426	418	0.98	10.6	0.000429	0.94	34.624	0.326	0.0572	0.0013	0.0286	0.0003	181.8	1.7
1.3	III	560	466	0.83	6.8	0.001724	3.814	70.991	0.773	0.0780	0.0024	0.0135	0.0001	86.8	0.9
2.1	I	274	232	0.85	9.0	0.001932	2.34	33.170	0.513	0.0685	0.0019	0.0294	0.0005	187.1	2.9
2.2	II	186	122	0.65	5.0	0.000812	1.26	41.435	0.733	0.0590	0.0015	0.0238	0.0004	151.8	2.7
4.1	III	269	146	0.54	4	0.001103	2.233	65.743	1.286	0.0668	0.0017	0.0149	0.0003	95.2	1.9
4.2	II	50	41	0.81	1	0.001852	5.363	38.622	1.114	0.0916	0.0042	0.0245	0.0007	156.1	4.5
4.3	I	396	655	1.66	10.1	0.001968	2.550	33.706	0.590	0.0701	0.0040	0.0289	0.0005	183.7	3.2
5.1	I	1141	958	0.84	36	0.000412	0.208	33.469	0.396	0.0516	0.0005	0.0298	0.0004	189.4	2.2
5.2	III	537	70	0.13	6.1	0.001844	1.907	75.104	0.711	0.0628	0.0013	0.0131	0.0002	83.7	1.0
7.1	III	338	1918	5.67	4	0.007927	14.934	176.790	3.217	0.1640	0.0039	0.0048	0.0001	30.9	0.6
7.2	II	554	404	0.73	15	0.000323	0.483	42.780	0.661	0.0529	0.0010	0.0233	0.0004	148.2	2.3
7.3	III	447	1158	2.59	4.1	0.003730	8.409	94.256	2.081	0.1139	0.0137	0.0097	0.0003	62.3	1.9
8.1	III	283	243	0.86	4	0.002842	5.66	81.589	1.472	0.0910	0.0021	0.0116	0.0002	74.1	1.4
8.2	II	147	86	0.58	4	0.002147	3.36	40.163	0.905	0.0757	0.0025	0.0241	0.0006	153.3	3.5

Notes: 1. Uncertainties given at the 1σ level. 2. Error in AS3 reference zircon calibration was 1.33% and 0.45% for the two analytical sessions (not included in above errors but required when comparing data from different mounts). 3. f_{206} % denotes the percentage of ^{206}Pb that is common Pb. 4. Correction for common Pb made using the measured $^{238}U/^{206}Pb$ and $^{207}Pb/^{206}Pb$ values following Tera & Wasserburg (1972), as outlined in Williams (1998). Gr.: grain.

Pb analyses. The REE analyses were carried out using SHRIMP II in energy-filtering mode, following techniques described in Ireland & Wlotzka (1992) and Hoskin & Ireland (2000). The data are set out in Table 3 and shown in Figures 7a and b. The patterns are dominantly those recorded in igneous zircon (for example, Hoskin & Ireland 2000), except for two of the light mottled CL zones (spots 7.1 and 8.1; Type III), which show a significant LREE enrichment, coinciding in some crystals with a notable enrichment in Th (Table 2, Fig. 6). This LREE enrichment may well be explained by a locally higher amount of fluids during the recrystallization processes and, in some cases, by a local chemical re-equilibration originating by the breakdown of a REE-rich phase, such as allanite or clinozoisite.

The examples of igneous zircon of mafic rocks analyzed until now, mainly corresponding to Fe–Ti-rich gabbroic protoliths, present a negative Eu anomaly in their REE pattern normalized to chondritic values. This anomaly has been interpreted by Rubatto & Hermann (2003) as due to crystallization of zircon after the development of feldspar, which acted as a sink for Eu. The igneous zircon from the Lugros eclogites does not present such a negative Eu anomaly. This difference could be explained by the fact that zircon in these rocks did not develop from a residual magmatic fluid, depleted in Eu by previous crystallization of feldspar, but it crystallized in coexistence with plagioclase, in a gabbroic protolith that even presents a slightly positive bulk-rock Eu anomaly (Eu/Eu* = 1.15).

The recrystallization process, visible in the CL images (Fig. 4), has not significantly disturbed the igneous REE patterns, except for the previously mentioned LREE enrichment in some areas. Nevertheless, in each crystal, the REE content from Lu to Eu is normally lower in the recrystallized zones than in the corresponding oscillatory-zoned rim (Fig. 7a). The extent of this decrease in REE concentrations is normally more notable in the Type-III than the Type-II recrystallized areas, as shown by their REE average values (Fig. 7b). Moreover, in the recrystallized areas (Figs. 7a, b), a change in REE pattern in the interval from Eu to Ce due to a slight increase in LREE is accompanied by a relative minimum in Eu, although this increase was not as notable as for spots 7.1 and 8.1. These variations in the REE contents of the recrystallized zones of the zircon, in comparison to their igneous zones, may be interpreted as being due to REE re-equilibration of the igneous zircon by processes of metamorphic recrystallization, favored by fluids filling the vesicles in these crystals.

Similar variations in the REE patterns between protoliths of igneous zircon and their recrystallized areas were reported by Hoskin & Black (2000) for metagranitic rocks, partially recrystallized during granulite-facies metamorphism. In eclogites from Monviso, in the Western Alps, some of igneous zircon that, according to Rubatto & Hermann (2003), survived undisturbed together with the eclogitic paragenesis, show internal zones of bright CL alteration, yielding apparent younger ages than those of the protolith; they recall

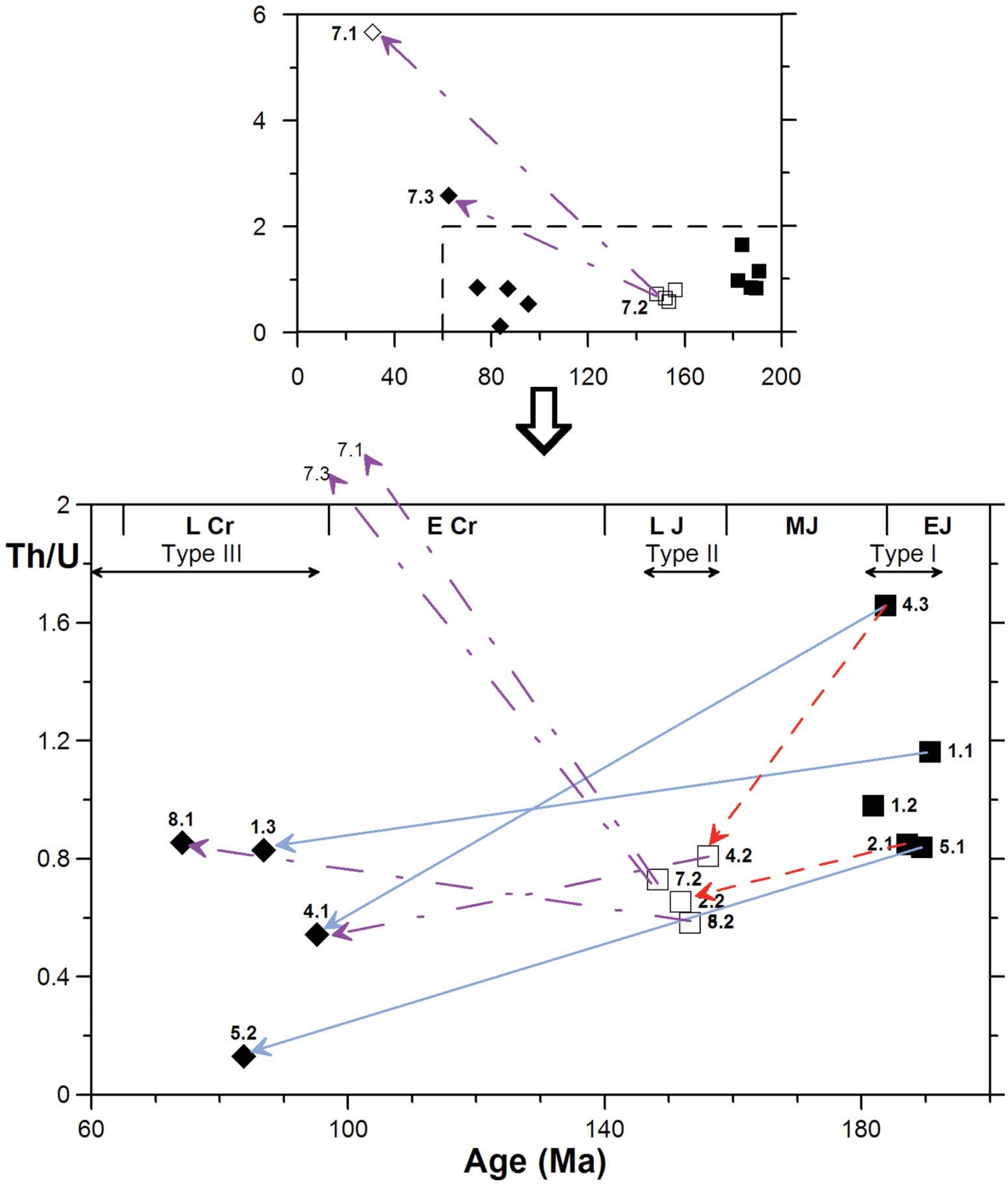

FIG. 6. Th/U value of the different crystals of zircon dated by SHRIMP in this study and represented in Figure 4. The variations in Th/U among the various zones texturally distinguished in these zircon crystals are indicated by differently colored arrows joining spots dated in the same crystal. The numbers of these spots correspond to those in Figure 4 and Tables 2 and 3. Key for symbols and abbreviations: full squares: type-I areas, empty squares: type-II areas, full and empty diamonds: type-III areas. L Cr: late Cretaceous, E Cr: early Cretaceous, L J: Late Jurassic, M J: Mid-Jurassic, E J: Early Jurassic.

some Alpine recrystallization-induced textures in the Lugros suite of zircon crystals, but it is not possible to compare their REE patterns, as these were not published in that paper. Other cases of zircon newly formed in eclogitic conditions, as an overgrowth on igneous zircon, or as neoblasts in eclogitic veins, formed in presence of hydrous fluids, present a HREE depletion indicative of their blastesis in equilibrium with a garnet (Rubatto & Hermann 2003). This HREE depletion is obviously not present in the REE patterns of the recrystallized areas of zircon in the Lugros eclogites, which mainly tend to mimic the REE patterns of the igneous protoliths from which they were derived.

In addition to the minor changes in the REE patterns previously described, other trace elements, such as Y and Hf, present in the recrystallized areas evidence of Y depletion and Hf enrichment, which are similar to the changes reported by Hoskin & Black (2000) and Vavra *et al.* (1996) in recrystallized areas of igneous zircon in granulite-facies conditions. These changes in Y and Hf contents can be seen in Table 3 if one compares the igneous areas, type I, with the corresponding recrystallized areas, type II or III, in the different analyzed crystals, with the exception of spot 1.3, which presents an anomalous pattern of behavior for a recrystallized zone, with Y increased and Hf decreased. The chemical anomalies presented by these elements between the recrystallized area, spot 1.3, and the igneous protolith, spot 1.1, are also corroborated by the increase in REE contents (Table 3), as well as in U and Th contents (Table 2).

Geological Interpretation of the Radiometric Ages of the Zircon

The SHRIMP U–Pb dating of the oscillatory zoned zircon (type I in Figs. 3, 4) constrains the age of the basic magmatism to be Early to Middle Jurassic. The lack of inherited cores in some of the igneous zircon crystals indicates that these mantle-derived magmas did not assimilate crustal rocks. This fact is consistent with the geochemical characteristics of the hosting eclogites, which correspond to an E–MORB-type magma (Puga *et al.* 1995, 2002a, Puga, in press).

Other radiometric dates of this episode of magmatism have been reported in Table 1. They correspond to whole-rock data and to results on mineral separates of gabbros and basalts of the BOA, from Cóbdar and Lubrin, two nearby outcrops in Sierra de Filabres that locally preserve the igneous parageneses (Fig. 1). An intercumulus biotite from a Cóbdar metagabbro yielded an ^{40}Ar–^{39}Ar age corresponding to the Triassic–Jurassic boundary. This date was considered to either constrain the onset of magmatic activity in rift conditions in this area, or the intrusion of basic magma at the limit between the ocean floor and the continental crust, because this rock presents some indications of crustal assimilation (Puga *et al.* 1989b, 2002a). K–Ar data for two other intrusive rocks from the same outcrop yielded a Middle Jurassic age (Portugal *et al.* 1988). From the Lubrin outcrop, a Rb–Sr total-rock isochron for metagabbroic cumulates similar to those dated from Cóbdar (Morten *et al.* 1987) yielded an Upper Jurassic

TABLE 3. SELECTED REE AND OTHER TRACE-ELEMENT DATA FOR ZIRCON SHOWN IN FIGURE 4 AND REFERRED TO IN FIGURES 6 AND 7

	1.1	1.3	2.2	4.1	5.1	5.2	7.1	7.2	7.3	8.1	8.2	c1norm
Y ppm	8815	13130	7248	1605	10769	4046	1654	4636	2525	1812	2998	4.6400
Hf	8844	8360	8686	6271	8568	8595	8638	5623	8265	8995	8827	0.103
La	0.01	0.17	0.01	0.01	0.01	0.01	1.56	0.02	0.02	7.73	0.02	0.2370
Ce	19.93	72.84	62.31	11.57	81.19	12.69	21.16	38.06	20.78	33.48	13.48	0.6130
Pr	0.20	0.64	0.22	0.08	0.34	0.10	0.95	0.11	0.07	3.52	0.03	0.0928
Nd	4.04	14.19	4.78	1.17	7.19	1.88	5.79	2.06	1.15	17.74	0.62	0.4570
Sm	3.87	13.06	5.34	1.17	7.60	2.02	6.22	2.06	1.25	18.90	0.64	0.1480
Eu	4.67	15.24	4.14	0.57	9.81	2.57	0.60	1.36	0.82	1.16	1.16	0.0563
Gd	75	181	102	16	159	41	15	41	26	24	25	0.1990
Tb	41	93	46	7	65	19	6	21	11	10	13	0.0361
Dy	594	1298	609	95	838	266	89	303	162	125	203	0.2460
Ho	221	454	224	38	301	109	42	121	67	50	87	0.0546
Er	924	1321	992	197	1276	553	207	484	353	257	428	0.1600
Tm	236	404	205	50	256	131	79	136	86	61	99	0.0247
Yb	2181	3672	1629	480	1985	1214	935	1195	844	561	849	0.1610
Lu	342	519	241	86	285	208	194	199	157	95	136	0.0246
Type	I	III	II	III	I	III	III	II	III	III	II	

Normalization values after Sun & McDonough (1989).

age (Hebeda *et al.* 1980), whereas a biotite separate yielded a Middle Jurassic age (De Jong 2003). The *ca.* 30 Ma discrepancy between the Rb–Sr data and the ^{40}Ar–^{39}Ar biotite data may be due to the presence of excess ^{40}Ar incorporated in this mineral during metamorphism, according to De Jong (2003). Nevertheless, our present finding of an Early to Middle Jurassic date for zircon from metagabbros at Lugros suggest that the Lubrin and Cóbdar metagabbros may also have been intruded during the Early and Middle Jurassic, as their K–Ar and ^{40}Ar–^{39}Ar dates indicate.

The four Middle and Late Jurassic (~150 Ma) results corresponding to SHRIMP U–Pb dating of type-II areas of the Lugros zircon may be interpreted as due to a first stage of recrystallization, which produced the now CL-homogeneous grey areas within the previously zoned components (Figs. 3, 4). This first stage of recrystallization may have originated by ocean-floor metamorphism that the host gabbros underwent during and after the development of the overlying volcanic sequence. A typical mineral of this pre-Alpine oceanic metamorphism is a brown amphibole, very rich in Ti, the relics of which are present in the Lugros eclogites and the other metabasic outcrops of the BOA (Puga *et al*. 1999b, 2002b). This type of amphibole, filling millimetric veins in ophiolitic pillow metabasalts from Cóbdar, has been dated by ^{40}Ar–^{39}Ar laser probe at 158 ± 4 Ma (Table 1).

The Late Cretaceous to Paleocene apparent ages yielded by the type-III areas of zircon presumably is related to the Eo-alpine metamorphic event that caused the eclogite facies in their host gabbros. These irregular luminescent areas seem to have developed by metamorphic recrystallization of the igneous zircon facilitated by the fluids included in pre-existing vesicles corresponding to the present holes. According to Vavra *et al.* (1996), the zircon recrystallizes during episodes of increasing temperature, because this process requires a relatively high activation-energy. Therefore, this recrystallization process would be expected to occur during the prograde stage of the Eo-alpine episode of subduction. The Late Cretaceous apparent ages would represent a maximum age for the Eo-alpine climax. This suggestion is in agreement with the Late Cretaceous K–Ar age previously done on glaucophane of an amphibolitized basalt from Cóbdar (Table 1). This amphibole is the most characteristic mineral formed during the retrograde Eo-alpine stage, although it can be also found as inclusions in omphacite and almandine of the Eo-alpine metamorphic climax. To this Eo-alpine event might also correspond the phengite from an amphibolite from Lubrin (Table 1), dated as Late Cretaceous by ^{40}Ar–^{39}Ar, if this mineral really does not have the excess Ar proposed by De Jong (2003).

The youngest apparent SHRIMP U–Pb ages, at about 50 and 30 Ma, could be related to the less pervasive processes of recrystallization associated with the Meso-alpine event, which led to the formation of some albite–epidote amphibolite assemblages in the Lugros eclogites. Several ^{40}Ar–^{39}Ar and K–Ar ages from 50 to 25 Ma, presented in Table 1, correspond to sodic-calcic amphiboles and phengite characteristic of the Meso-alpine albite–epidote amphibolite facies. No SHRIMP U–Pb ages corresponding to the Neo-alpine event was encountered in the zircon of the Lugros eclogites.

It is common that zircon from a gabbro transformed to an eclogite does not record a notable overgrowth. This is particularly the case if the zircon is derived from an ocean-floor magma, which is very poor in Zr compared to basic magmas derived from the continental lithospheric mantle, or from other rock types that underwent metamorphism under granulite-facies conditions (Vavra *et al*. 1996, Roberts & Finger 1997). In general, the ophiolitic gabbros from the Alps, whose origin and chemical composition are similar to those from the BOA, contain relict igneous zircon undisturbed during the eclogitic event, *e.g.*, those of the Monviso eclogites (Rubatto & Hermann 2003). Furthermore, in these gabbros, the zircon grains are less commonly overgrown during the eclogitization process than those in genetically associated rocks recrystallized during the same metamorphic process (Rubatto *et al*. 1998). In a detailed study designed to date the ophiolitic eclogites in the Zermatt–Saas–Fee zone, Rubatto *et al.* (1998) found one single overgrown crystal of zircon in the Mellichen metagabbro; this crystal records two ages, *ca.* 90 and 70 Ma, which the authors dismissed as not significant event(s) owing to their unique and non-repeated nature. A third analysis on another segment of the rim of the same grain yielded an equally unique and non-repeated U–Pb age, *ca.* 50 Ma. The latter was interpreted as being the maximum age of the Eo-alpine metamorphism owing to the similarity with other U–Pb ages yielded by different ophiolitic lithotypes in the same zone. Thus, we conclude that the most decisive factor in the development of zircon overgrowths, or newly formed zircon crystals, during the different stages of metamorphic events is most probably the availability of Zr during each stage of blastesis and the competition that might arise for this element between zircon and the other minerals formed in each paragenesis.

The fact that new zircon did not overgrow the igneous relict zircon in the Lugros rocks under the eclogite-facies conditions is probably a consequence of the lack of available Zr during the Eo-alpine metamorphism. This element, derived in sparse amounts from the breakdown of primary ilmenite, must have been preferentially incorporated into other minerals of the eclogitic paragenesis, such as rutile, garnet and omphacite. Similarly, neither was the zircon from the Lugros eclogites overgrown during the Meso-alpine event, suggesting a preferential incorporation of the Zr liberated from garnet and omphacite breakdown into the amphibole of the new amphibolite paragenesis. Amphibole is a phase that can readily incorporate Zr, even more so than garnet (*cf.* Fraser *et al.* 1997). Under these chemical constraints, relics of igneous zircon may only react under the physical conditions of metamorphism where the threshold of the activation energy of recrystallization is overcome.

DISCUSSION ON THE AGE OF THE ECLOGITIC METAMORPHISM

The data presented in Figures 4 to 6 and Table 2 are the first SHRIMP U–Pb data on zircon in eclogites from the Mulhacén Complex ophiolites. The SHRIMP data obtained by analyses of the Type-III zircon areas in Lugros eclogites did not yield any coherent age-data corresponding to newly formed zircon during the Alpine metamorphic period (Fig. 5). Nevertheless, the apparent Late Cretaceous to Paleocene ages yielded by these recrystallized areas indicate that the recrystallization process, which gave place to the changes in textures and chemical composition shown in Figures 3 to 7, took place mainly during the prograde stage of the Eo-alpine metamorphic event that created their host eclogites. This conclusion is in agreement with the late Cretaceous K–Ar age obtained on glaucophane of the Cóbdar amphibolitized eclogites (Table 1), which is the only type of amphibole formed in the BOA metabasites during the Eo-alpine event. The Eocene–Oligocene K–Ar and Ar–Ar radiometric ages reported in Table 1 correspond to sodic-calcic and calcic amphiboles and white mica of the Meso-alpine albite–epidote amphibolite paragenesis, which clearly postdates the eclogitic paragenesis, which it partially replaces. Finally, the K–Ar, Ar–Ar and U–Pb ages reported in Table 1 correspond to the Miocene Neo-alpine stage of recrystallization of the earlier parageneses, which involves very localized blastesis under greenschist-facies conditions, mainly of white mica and actinolite in metabasic rocks, and zircon in boudinaged veins of metaclinopyroxenite within serpentinites.

The Neo-alpine retrogression blastesis in the MC has been attributed to the tectonic processes linked to the extensional collapse of the Betic orogen (Platt & Vissers 1989, Monié *et al.* 1991). It has been also related to the post-orogenic calc-alkaline magmatism and coeval hydrothermal activity, which developed in the Betic Cordillera between 15 and 7 Ma (Bellon *et al.* 1983). This type of magmatism may have been genetically related to a Neo-alpine continental subduction (Araña & Vegas 1974, Morales *et al.* 1999), although other genetic conditions might also explain its origin (Puga 1980, Torres Roldán *et al.* 1986, Larouzière *et al.* 1988, Turner *et al.* 1999). In any case, this hypothetical stage of Miocene subduction would not be related to the intra-oceanic Late Cretaceous to Early Tertiary subduction process that consumed the majority of the Jurassic ocean floor forming the western end of the Tethys ocean, and that caused the eclogite facies in the Betic Cordillera and other Alpine Ranges. Nevertheless, López Sánchez-Vizcaino *et al.* (2001) have reported a SHRIMP U–Pb zircon date of 15 ± 0.6 Ma (Table 1) from a boudin of metaclinopyroxenite within serpentinite from the Cerro del Almirez, which forms part of the BOA. They interpreted the zircon as having formed during the eclogite-facies metamorphism that affected the ultramafic host-rocks (Puga *et al.* 1997, 1999a, Trommsdorff *et al.* 1998). Their assignment of a mid-Miocene age to the eclogitic paragenesis is based on the fact that some of the dated zircon crystals contain inclusions of antigorite, which they considered as being paragenetic and formed during the high-pressure metamorphic climax in the enclosing ultramafic assemblages. This inference may be incorrect, however, because antigorite in these rocks is commonly a retrograde phase replacing the typical Eo-alpine peak minerals such as forsterite, orthopyroxene, titanclinohumite and diopside (Puga *et al.* 1999a). Thus, on the basis of this disputable textural observation, López Sánchez-Vizcaino *et al.* (2001) concluded that the dated zircon corresponds to the eclogite paragenesis, and that the subduction process causing the high-P metamorphism in the MC of the Nevado–Filábride domain lasted at least until the mid-Miocene.

An alternative hypothesis concerning the origin of this zircon might be that it formed as a consequence of breakdown of some Zr-bearing minerals, forming the host clinopyroxenite during the stage of Neo-alpine decompression, which was characterized by the circulation of abundant hydrothermal fluids. The Zr-bearing phases, which would be unstable under these conditions, may be the relics of mantle-derived clinopyroxene, which are common in this rock type and contain ilmenite lamellae, and the titanclinohumite of the eclogitic paragenesis (Puga *et al.* 1999a). This hypothesis is also supported by the observation of López Sanchez-Vizcaino *et al.* (2001), that the dated zircon "is found in small domains near titanian clinohumite or together with its breakdown products".

The assumption that the mid-Miocene zircon in the boudinaged metapyroxenite vein was developed under eclogite-facies conditions led López-Sanchez Vizcaino *et al.* (2001) and De Jong (2003) to deduce much faster rates of exhumation, for the host rocks of the zircon, than might have been arrived at if the zircon had developed during a retrograde stage with respect to the peak metamorphic pressure, or else had a hydrothermal origin. Geological and experimental studies do in fact allow for both these types of origin for the zircon (*cf.* Wayne & Sinha 1988, Rubin *et al.* 1989, Fraser *et al.* 1997, Roberts & Finger 1997, Watson *et al.* 1997, Rubatto *et al.* 1999, Nesbitt *et al.* 1999). These investigators, amongst others, showed that Zr can be incorporated into a rock by hydrothermal fluids, or be remobilized at the mineral scale by a metamorphic fluid phase during the breakdown of common Zr-bearing metamorphic minerals forming part of an eclogitic or granulitic paragenesis. The destabilization of these phases occurs more often during processes of retrograde metamorphism, which is why the so-called "metamorphic zircon ages" do not necessarily coincide with the

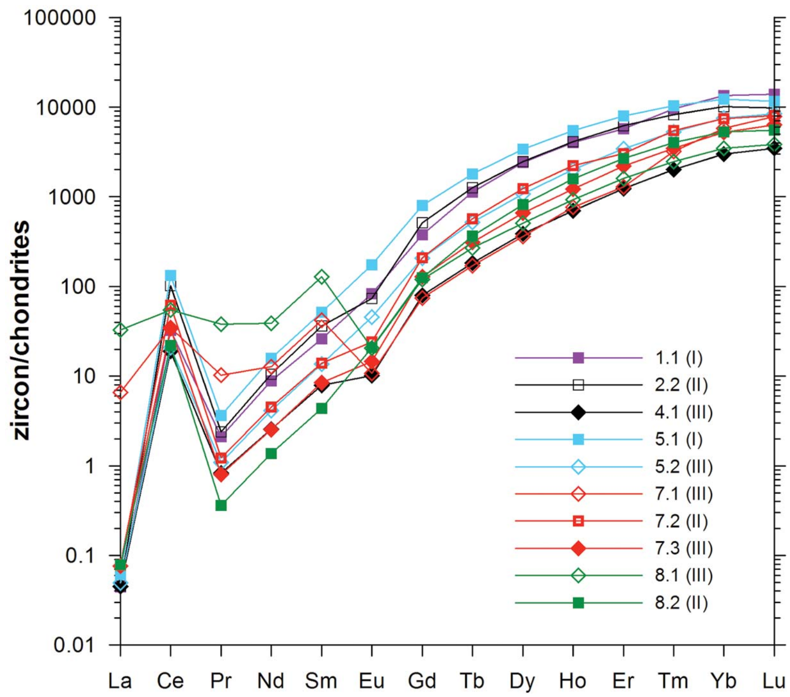

FIG. 7a. REE patterns of some spots of zircon crystals represented in Figure 4. Numerical data are given in Table 3, together with Hf and Y content of these zircon crystals. The textural type of the recrystallized areas is indicated in the legend for each spot by the Roman numeral (in parentheses), together with the number of the analysis.

P–T peak of metamorphism (*cf*. Roberts & Finger 1997, Desmons *et al*. 1999).

Thus, we consider, together with other authors (*cf.* Chalouan & Michard 2004), that the eclogitic metamorphism that affected the BOA and other units of the MC must have developed during Late Cretaceous to Paleocene Eo-alpine subduction, and that the mid-Miocene zircon identified in the Almirez metapyroxenites by López Sánchez-Vizcaíno *et al*. (2001) is more probably related to the extensional collapse that affected the Betic Cordillera during the Miocene.

CONCLUSIONS

1. The U–Pb SHRIMP dating of subidiomorphic and oscillatory-zoned areas (Type I) of zircon from the Lugros ophiolitic eclogites, led us to establish an Early to Mid-Jurassic age of 184 ± 4 Ma for the igneous crystallization of the basic protolith, whereas we interpret the grey homogeneous areas (Type II) of the same zircon crystals as belonging to a Mid- to Late-Jurassic stage of recrystallization caused by the ocean-floor metamorphism, which affected these rocks during the development of the overlying volcanic sequence.

2. The analyses of the Type-III zircon areas did not yield any coherent age-data, but the Late Cretaceous to Paleocene apparent ages of these CL bright areas correspond to an episode of recrystallization, which most probably occurred during the prograde stage of the Eo-alpine metamorphic event in which the eclogite paragenesis developed.

3. The REE patterns of the texturally differentiated areas in the zircon are all very similar, and correspond mainly to the chemical composition of igneous zircon crystals. Nevertheless, the contents of the heavy and middle rare-earth elements appear to decrease during the recrystallization processes, and the light REE were in some cases depleted, and in others clearly enriched, with respect to the pattern of the oscillatory-zoned rim.

4. The lack of a newly formed rim of zircon in these partly amphibolitized eclogites must be due to the preferential incorporation of the scarce Zr contained in the igneous phases of the oceanic gabbroic protolith into other metamorphic minerals, such as rutile, almandine, omphacite and amphibole, as well as to the absence during metamorphism of additional Zr contributed by fluids external to the system.

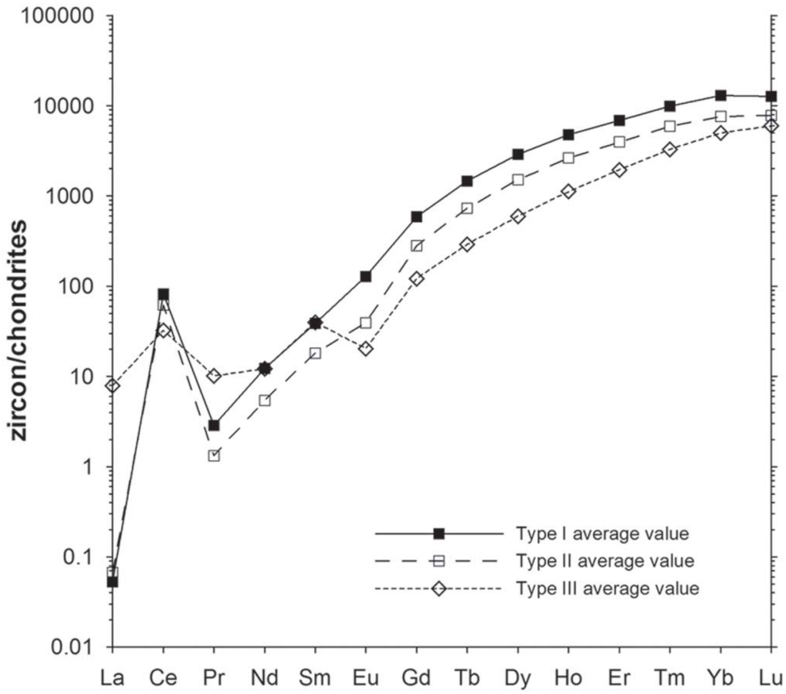

FIG. 7b. Comparison of the average REE patterns of the various types of areas distinguished by CL images in the crystals of zircon.

5. The preferential location of the brightest recrystallized zones around internal holes, interpreted as preexisting fluid-filled vesicles, suggests an important role for ocean-floor fluids, which they likely contained, on the processes of metamorphic recrystallization of the igneous zircon and on the origin of their peculiar "corona", "cloud of smoke" and "flame" textures.

6. The preferential effect of metamorphic recrystallization in the inner parts of the zircon crystals, mainly in the areas surrounding holes, rather than at their periphery, is the cause of an apparent inversion of age, which decreases from the preserved igneous rim to the recrystallized core.

ACKNOWLEDGEMENTS

Dugald Carmichael's rigorous and innovative research has exerted a very positive influence on our work on metamorphic rocks, and it is with great pleasure that we dedicate this paper to him on the occasion of his retirement. We are indebted to Bill Davis, Greg Dunning, Marc St-Onge, Jacqueline Desmons and Robert F. Martin for their careful and pertinent critical comments, which have helped us greatly in improving the text. E.P. also thanks Dr. J. Trout for revising the English of a first version of the text, and A. Díaz Puga for his valuable help in processing the figures. This project was funded by Project BTE2002–10412–E of the Spanish Ministry of Science and Technology, cofinanced with the FEDER funds, and by Research Group RNM 333 of the Junta de Andalucía.

REFERENCES

ANDRIEUX, J., FRIZON DE LAMOTTE, D. & BRAUD, J. (1989): A structural scheme for the Western Mediterranean area in Jurassic and Early Cretaceous times. *Geodinamica Acta* **3**, 5-15.

ARAÑA, V. & VEGAS, R. (1974): Plate tectonics and volcanism in the Gibraltar arc. *Tectonophys.* **24**, 197-212.

BECCALUVA, L., DAL PIAZ, G.V. & MACCIOTA, G. (1984): Transitional to normal MORB affinities in ophiolitic metabasites from the Zermatt–Saas, Combin and Antrona units, Western Alps: implications for the paleogeographic evolution of the Western Tethyan Basin. *Geol. in Mijnbouw* **63**, 165-177.

BELLON, H., BORDET, P. & MONTENAT, C. (1983): Chronologie du magmatisme néogène des Cordillères bétiques (Espagne méridionale). *Soc. Geol. Fr., Bull.* **25**, 205-217.

CHALOUAN, A. & MICHARD, A. (2004): The Alpine Rif Belt (Morocco): a case of mountain building in a subduction–subduction–transform fault triple junction. *Pure Appl. Geophys.* **161**, 489-519.

DAL PIAZ, G.V. (1974): Le métamorphisme de haute pression et basse température dans l'evolution structurale du bassin ophiolitique alpino-apenninique. *Schweiz. Mineral. Petrogr. Mitt.* **54**, 399-424.

DE JONG, K. (2003): Very fast exhumation of high-pressure metamorphic rocks with excess ^{40}Ar and inherited ^{87}Sr, Betic Cordilleras, southern Spain. *Lithos* **70**, 91-110.

________, WIJBRANS, J.R. & FERAUD, G. (1992): Repeated thermal resetting of phengites in the Mulhacén Complex (Betic Zone, southeastern Spain), shown by ^{40}Ar/^{39}Ar step heating and single grain laser probe dating. *Earth Planet. Sci. Lett.* **110**, 173-191.

DESMONS, J. (1989): Different metamorphic evolutions in the Alpine–Apenninic ophiolites (France – Italy – Switzerland – Austria). *Chem. Geol.* **77**, 229-250.

________, COMPAGNONI, R. & CORTESOGNO, L., with the collaboration of FREY, M., GAGGERO, L., DALLAGIOVANNA, G., SENO, S. & RADELLI, L. (1999): Alpine metamorphism of the Western Alps. II. High P/T and related pre-greenschist metamorphism. *Schweiz. Mineral. Petrogr. Mitt.* **79**, 111-134.

DEWEY, J.F., HELMAN, M.L., TURCO, E., HUTTON, D.H.W. & KNOTT, S.D. (1989): Kinematics of the western Mediterranean. *In* Alpine Tectonics (N.P. Coward, D. Dietrich & R.G. Park, eds.). *Geol. Soc., Spec. Publ.* **45**, 265-283.

________, PITMAN, W.C., III., RYAN, W.B.F. & BONIN, J. (1973): Plate tectonics and the evolution of the Alpine System. *Geol. Soc. Am., Bull.* **84**, 3137-3180.

DIETRICH, V.J. (1980): The distribution of ophiolites in the Alps. *Ofioliti*, *Spec. Issue* **1**, 7-51.

FAVRE, P. & STAMPFLI, G.M. (1992): From rifting to passive margin: the examples of the Red Sea, central Atlantic and Alpine Tethys. *Tectonophys.* **215**, 69-97.

FRASER, G., ELLIS, D. & EGGINS, S. (1997): Zirconium abundance in granulite-facies minerals, with implication for zircon geochronology in high-grade rocks. *Geology* **25**, 607-610.

GUERRERA, F., MARTIN-ALGARRA, A. & PERRONE, V. (1993): Late Oligocene-Miocene syn-/-late-orogenic succesions in western and central Mediterranean chains from the Betic Cordillera to the southern Apennines. *Terra Nova* **5**, 525-544.

HEBEDA, E.H., BOELRIJK, N.A.I.M., PRIEM, H.N.A., VERDURMEN, E.A.TH., VERSCHURE, R.H. & SIMON, O.J. (1980): Excess radiogenic Ar and undisturbed Rb–Sr systems in basic intrusives subjected to Alpine metamorphism in southeastern Spain. *Earth Planet. Sci. Lett.* **47**, 81-90.

HOSKIN, P.W.O. & BLACK, L.P. (2000): Metamorphic zircon formation by solid-state recrystallization of protolith igneous zircon. *J. Metamorph. Geol.* **18**, 423-439.

________ & IRELAND, T.R. (2000): Rare earth element chemistry of zircon and its use as a provenance indicator. *Geology* **28**, 627-630.

IRELAND, T.R. & WLOTZKA, F. (1992): The oldest zircons in the solar system. *Earth Planet. Sci. Lett.* **109**, 1-10.

LAROUZIÈRE, F.D., DE BOLZE, J., BORDET, P., HERNANDEZ, H., MONTENAT, C. & OTT D'ESTEVOU, P. (1988): The Betic segment of the lithospheric Trans-Alboran shear zone during the Late Miocene. *Tectonophys.* **152**, 41-52.

LÓPEZ SÁNCHEZ-VIZCAÍNO, V., RUBATTO, D., GÓMEZ-PUGNAIRE, M.T., TROMMSDORFF, V. & MÜNTENER, O. (2001): Middle Miocene high-pressure metamorphism and fast exhumation of the Nevado–Filábride Complex, SE Spain. *Terra Nova* **13**, 327-332.

MICHARD, A., GOFFÉ, B., CHALOUAN, A. & SADDIQUI, O. (1991): Les corrélations entre les Chaînes bético-rifaines et les Alpes et leurs conséquences. *Soc. Géol. Fr., Bull.* **162**, 1151-1160.

MONIÉ, P., GALINDO-ZALDÍVAR, J., GONZÁLEZ-LODEIRO, F., GOFFÉ, B. & JABALOY, A. (1991): ^{40}Ar/^{39}Ar geochronology of Alpine tectonism in the Betic Cordilleras (southern Spain). *J. Geol. Soc. London* **148**, 289-297.

MORALES, J., SERRANO, I., JABALOY, A., GALINDO-ZALDIVAR, J., ZHAO, D., TORCAL, F., VIDAL, F. & GONZALEZ-LODEIRO, F. (1999): Active continental subduction beneath the Betic Cordillera and the Alborán Sea. *Geology* **27**, 735-738.

MORATA, D., PUGA, E., DEMANT, A. & AGUIRRE, L. (1997): Geochemistry and tectonic setting of the "ophites" from the external zones of the Betic Cordilleras (southern Spain). *Estud. Geol.* **53**, 107-120.

MORTEN, L., BARGOSSI, G.M., MARTÍNEZ, J.M.M., PUGA, E. & DÍAZ DE FEDERICO, A. (1987): Metagabbro and associated eclogites in the Lubrin area, Nevado–Filabride Complex, Spain. *J. Metamorph. Geol.* **5**, 155-174.

NASLUND, H.R. (1984): Supersaturation and crystal growth in the roof-zone of the Skaergaard magma chamber. *Contrib. Mineral. Petrol.* **86**, 89-93.

NESBITT, R.W., PASCUAL, E., FANNING, C.M., TOSCANO, M., SAEZ, R. & ALMODOVAR, G.R. (1999): U–Pb dating of stockwork zircons from the eastern Iberian Pyrite Belt. *J. Geol. Soc. London* **156**, 7-10.

NIETO, J.M., JAGOUTZ, E., PUGA, E. & DÍAZ DE FEDERICO, A. (1997): Sm–Nd isotopic disequilibrium in eclogites from the Mulhacén Complex (Betic Cordillera, Spain). *Terra Nova* **9**, 22.

PIDGEON, R.T. (1992): Recrystallization of oscillatory zoned zircon – some geochronological and petrological implications. *Contrib. Mineral. Petrol.* **110**, 463-472.

PLATT, J.P. & VISSERS, R.L.M. (1989): Extensional collapse of thickened continental lithosphere: a working hypothesis for the Alboran Sea and the Gibraltar arc. *Geology* **17**, 540-543.

PORTUGAL FERREIRA, M., FERREIRA, J. D., PUGA, E. & DÍAZ DE FEDERICO, A. (1988): Geochronological contribution to the petrogenetic picture of the Betic Chain (SE Spain). *II Congr. Geol. Esp. Comunicaciones* **2**, 55-58.

PUGA, E. (1980): Hypothèse sur la genèse des magmatismes calco-alcalins, intra-orogénique et post-orogénique alpins, dans les Cordillères Bétiques. *Bull. Soc. Geol. France* **7**(XXIII, 2), 243-250.

________ (1990): The Betic Ophiolitic Association (southeastern Spain). *Ofioliti* **15**, 97-117.

________ (in press): Update of the Betic Ophiolitic Association: the westernmost relic of the Alpine Tethys. *Tectonophys., CROP Spec. Vol.*

________, BODINIER, J.L., DÍAZ DE FEDERICO, A., MORTEN, L. & NIETO, J.M. (1997): Pseudo-spinifex meta-ultramafic rocks containing eclogitized rodingite dykes in the Betic Ophiolitic Association (SE Spain): evidence of Alpine subduction following an ocean-floor metasomatic process. *Quaderni di Geodinamica Alpina e Quaternaria* **4**, 98-99.

________, DÍAZ DE FEDERICO, A., BARGOSSI, G.M. & MORTEN, L. (1989b): The Nevado–Filabride metaophiolitic association in the Cóbdar region (Betic Cordillera, SE Spain): preservation of pillow structures and development of coronitic eclogites, *Geodin. Acta* **3**, 17-36.

________, ________ & DEMANT, A. (1995): The eclogitized pillows of the Betic Ophiolitic Association: relics of the Tethys ocean floor incorporated in the Alpine chain after subduction. *Terra Nova* **7**, 31-43.

________, ________ & NIETO, J.M. (2002a): Tecotono-stratigraphic subdivision and petrological characterisation of the deepest complexes of the Betic zone: a review. *Geodinamica. Acta* **15**, 23-43.

________, NIETO, J.M. & DIAZ DE FEDERICO, A. (2000): Contrasting P–T path in eclogites of the Betic Ophiolitic Association, Mulhacén Complex, southeastern Spain. *Can. Mineral*. **38**, 1137-1161.

________, ________, ________, BODINIER, J.L. & MORTEN, L. (1999a): Petrology and metamorphic evolution of ultramafic rocks and dolerite dykes of the Betic Ophiolitic Association (Mulhacén Complex, SE Spain): evidence of Eo-alpine subduction following an ocean-floor metasomatic process. *Lithos* **49**, 23-56.

________, ________, ________, PORTUGAL, M. & REYES, E. (1996): The intra-orogenic Soportújar Formation of the Mulhacén Complex: evidence for the polycyclic character of the Alpine orogeny in the Betic Cordilleras. *Eclogae Geol. Helv*. **89**, 129-162.

________, PORTUGAL, M., DÍAZ DE FEDERICO, A., BARGOSSI, G.M. & MORTEN, L. (1989a): The evolution of the magmatism in the external zones of the Betic Cordilleras during the Mesozoic. *Geodinamica. Acta* **3**, 253-266.

________, RUIZ CRUZ, M.D. & DIAZ DE FEDERICO, A. (1999b): Magnetite–silicate inclusions in olivine of ophiolitic metagabbros from the Mulhacén Complex, Betic Cordillera, southeastern Spain. *Can. Mineral.* **37**, 1191-1209.

________, ________ & ________ (2002b): Polymetamorphic amphibole veins in metabasalts from the Betic Ophiolitic Association at Cóbdar, southeastern Spain: relics of ocean-floor metamorphism preserved throughout the Alpine orogeny. *Can. Mineral*. **40**, 67-83.

________ & TORRES ROLDÁN, R.L. (1989): Geochemistry and age relationships of metamorphosed mafic sills from Sierra de Enmedio and Sierra de Carrascoy (Eastern Betic Zone, southeastern Spain). *Estud. Geol*. **45**, 325-336.

ROBERTS, M.P. & FINGER, F. (1997): Do U–Pb zircon ages from granulites reflect peak metamorphic conditions? *Geology* **25**, 319-322.

RUBATTO, D. (2002): Zircon trace element geochemistry: partitioning with garnet and the link between U–Pb ages and metamorphism. *Chem. Geol*. **184**, 123-138.

________, GEBAUER, D. & COMPAGNONI, R. (1999): Dating of eclogite facies zircons: the age of Alpine metamorphism in the Sesia–Lanzo zone (Western Alps). *Earth Planet. Sci. Lett*. **167**, 141-158.

________, ________ & FANNING, M. (1998): Jurassic formation and Eocene subduction on the Zermatt–Saas – Fee ophiolites: implications for the geodynamic evolution of the Central and Western Alps. *Contrib. Mineral. Petrol*. **132**, 269-287.

________ & HERMANN, J. (2003): Zircon formation during fluid circulation in eclogites (Monviso, Western Alps): implications for Zr and Hf budget in subduction zones. *Geochim. Cosmochim. Acta* **67**, 2173-2187.

RUBIN, J.N., HENRY, C.D. & PRICE, J.G. (1989). Hydrothermal zircons and zircon overgrowths, Sierra Blanca Peaks, Texas. *Am. Mineral*. **74**, 865-869.

RUIZ CRUZ, M.D., PUGA, E. & NIETO, J.M. (1999). Silicate and oxide exsolution in pseudo-spinifex olivine of the metaultramafic rocks of the Betic Ophiolitc Association: a TEM study. *Am. Mineralogist* **84**, 1915-1924.

SAUNDERS, A.D., NORRY, M.J. & TARNEY, J. (1988): Origin of MORB and chemically depleted mantle reservoirs: trace element constraint. *In* Oceanic and Continental Lithosphere: Similarities and Differences (M.A. Menzies & K.G. Cox, eds.). *J. Petrol., Lithosphere Spec. Issue*, 415-445.

SUN, S.-S. & MCDONOUGH, W.F. (1989): Chemical and isotopic systematics of oceanic basalts: implications for mantle composition and processes. *In* Magmatism in the Ocean Basins (A.D. Saunders & M.J. Norry, eds.). *Geol. Soc., Spec. Publ.* **42**, 313-345.

TERA, F. & WASSERBURG, G. (1972): U–Th–Pb systematics in three Apollo 14 basalts and the problem of initial Pb in lunar rocks. *Earth Planet. Sci. Lett.* **14**, 281-304.

TORRES ROLDÁN, R.L. (1979): The tectonic subdivision of the Betic Zone (Betic Cordilleras, southern Spain): its significance and one possible geotectonic scenario for the westernmost Alpine belt. *Am. J. Sci***. 279**, 19-51.

________, POLI, G. & PECCERILLO, A. (1986): An Early Miocene arc-tholeiitic dike event from the Alboran Sea: evidence for precollisional subduction and back-arc crustal extension in the westernmost Mediterranean. *Geol. Rundschau* **75**(1), 219-234.

TROMMSDORFF, V., LÓPEZ SÁNCHEZ-VIZCAÍNO, V., GÓMEZ-PUGNAIRE, M.T. & MÜNTENER, O. (1998): High pressure breakdown of antigorite to spinifex-textured olivine and orthopyroxene, SE Spain. *Contrib. Mineral. Petrol*. **132**, 139-148.

TURNER, S.P., PLATT, J.P., GEORGE, R.M.M., KELLEY, S.P., PEARSON, D.G. & NOWELL, G.M. (1999): Magmatism associated with orogenic collapse of the Betic–Alboran Domain, SE Spain. *J. Petrol.* **40**, 1011-1036.

VAVRA, G. (1990): On the kinematics of zircon growth and its petrogenetic significance: a cathodoluminescence study. *Contrib. Mineral. Petrol*. **106**, 90-99.

________, GEBAUER, D., SCHMID, R. & COMPSTON, W. (1996): Multiple zircon growth and recrystallization during polyphase Late Carboniferous to Triassic metamorphism in granulites of the Ivrea Zone (Southern Alps): an ion microprobe (SHRIMP) study. *Contrib. Mineral. Petrol*. **122**, 337-358.

VERA, J.-A. (2001): Evolution of the South Iberian continental margin. In Peri-Tethys Memoir 6: Peri-Tethyan Rift/Wrench Basins and Passive Margins (P.A. Ziegler, W. Cavazza, A.H.F. Robertson & S. Casquin-Soleau, eds.). *Mém. Muséum National d´Histoire Naturelle* **186**, 109-143.

WATSON, E.B., CHERNIAK, D.J., HANCHAR, J.M., HARRISON, T.M. & WARK, D.A. (1997): The incorporation of Pb into zircon. *Chem. Geol*. **141**, 19-31.

WAYNE, D.M. & SINHA, A.K. (1988): Physical and chemical response of zircons to deformation. *Contrib. Mineral. Petrol.* **98**, 109-121.

WILLIAMS, I.S. (1998): U–Th–Pb geochronology by ion microprobe. *In* Applications of Microanalytical Techniques to Understanding Mineralizing Processes (M.A. McKibben, W.C. Shanks III & W.I. Ridley, eds.). *Rev. Econ. Geol.* **7**, 1-35.

Received October 15, 2003, revised manuscript accepted October 14, 2004.